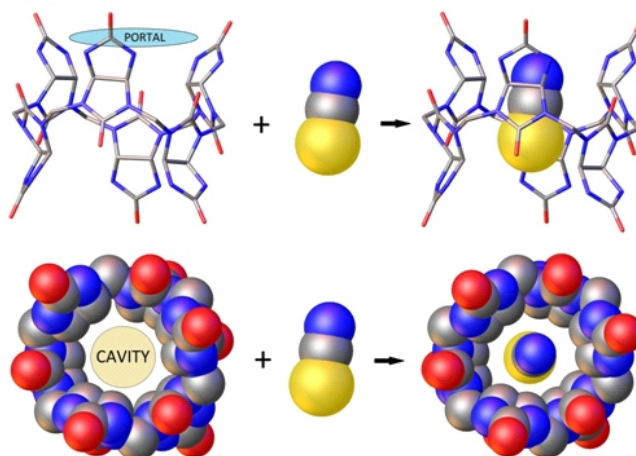




such inclusion compounds and are often studied as potential signaling molecules, catalysts, pharmaceutical transporters and "preservatives", or models for biological processes occurring at the surface of the membranes.

For this type of complexes, X-ray crystallography (among various NMR experiments) is usually the preferred method of structural analysis. However, the crystals usually have large unit cells with considerable quantities of solvents, which makes them somewhat similar to protein crystals regarding the data collection and refinement. Defects in crystal structure, such as a disorder in the solvent "area" around the hosts do occur quite often. A chemist is usually interested in remaining "non-solvent" parts of the structure, which means that some simplifications can be introduced. Practical aspects of X-ray diffraction studies on selected inclusion compounds of glycoluril-based macrocycles will be discussed in greater detail.

1. V. Havel and V. Sindelar, *ChemPlusChem* 2015.
2. L. Ustrnul, M. Babiak, P. Kulhanek and V. Sindelar, *J. Org. Chem.* 2016.



3. T. Fiala, L. Ludvikova, D. Heger, J. Svec, T. Slanina, L. Vetrakova, M. Babiak, M. Necas, P. Kulhanek, P. Klan and V. Sindelar, *JACS* 2016 (submitted).

## Session VII, Wednesday, September 14

SL8

### SOME NEW FINDINGS ABOUT THE POLYTIPIISM OF THE MINERAL CRONSTEDTITE

J. Hybler<sup>1</sup>, J. Sejkora<sup>2</sup>, M. Števkó<sup>3</sup>

<sup>1</sup>*Institute of Physics, Academy of Sciences of the Czech Republic, Na Slovance 2, CZ-182 21 Praha 8, Czech Republic*

<sup>2</sup>*Department of Mineralogy and Petrology, National Museum, Cirkusová 1740, CZ-193 00 Praha 9, Czech Republic*

<sup>3</sup>*Department of Mineralogy and Petrology, Faculty of Natural Sciences, Comenius University, Ilkovičova 6, SK-84215 Bratislava, Slovakia  
hybler@fzu.cz*

Polytypism of layer silicate cronstedtite ( $\text{Fe}^{2+}_{3-x}\text{Fe}^{3+}_x(\text{Si}_{2-x}\text{Fe}^{3+}_x)\text{O}_5(\text{OH})_4$ ,  $(0.5 < x < 0.8)$ ) was studied in numerous specimens from localities Eisleben (Germany), Pohled (Czech rep.) [1], Nižná Slaná (Slovakia) [2] by the four circle X-ray diffractometer with area detector. In addition, EMPA analyses of selected samples were done. Synthetic micrometer-size crystals were studied by electron diffraction tomography (EDT) [3]. These methods provide precession-like images of reciprocal lattice planes, relevant for the determination of OD subfamilies (A, B, C, D), and polytypes.

The rare  $1M$  polytype (subfamily A,  $a = 5.5033(3)$ ,  $b = 9.5289(6)$ ,  $c = 7.3328(5)$  Å,  $\beta = 104.493(7)^\circ$ , space group  $Cm$ ) was found as dominant in the synthetic run product [3]. A rare crystal from Eisleben allowed data collection and structure refinement [4]. More frequently it occurs in mixed crystals with  $3T$ , another, more abundant polytype of the subfamily A ( $a = 5.499(2)$ ,  $c = 21.260(8)$  Å, space group  $P3_1$ ). Such crystals were found in Pohled and Nižná Slaná samples. The newly discovered non-MDO polytype  $6T_2$  (subfamily A,  $a = 5.4976(3)$ ,  $c = 42.601(1)$  Å, space

group  $P3_1$ ) was found in Pohled [1]. Its structure was refined and stacking sequence determined [5]. Another rare  $2M_1$  polytype (subfamily A,  $a = 5.497(2)$ ,  $b = 9.507(2)$ ,  $c = 14.267(6)$  Å,  $\beta = 97.25(3)^\circ$ , space group  $Cc$ ) occurs in Pohled in mixed crystals with  $6T_2$ , and in synthetic samples either with  $3T$ , or isolated.

Polytypes of the subfamily A can be affected by twinning by reticular merohedry. The twinning operation -  $((2n-1) \times 60^\circ$  rotation parallel to the threefold axis) exchanges obverse/reverse settings of the  $R$  lattice of the rhombohedral subfamily A structure. The twinned crystals are common in Nižná Slaná ( $3T$  polytype), and rare in Pohled ( $6T_2$ ,  $3T + 1M$ ).

Mixed crystals of polytypes  $2H_1 + 2H_2$ , subfamily D, (lattice parameters of both polytypes  $a = 5.5002(4)$ ,  $c = 14.195(1)$  Å, space groups:  $P6_3cm$  ( $2H_1$ ),  $P6_3$  ( $2H_2$ )) were identified in Pohled, with various  $2H_1/2H_2$  proportions. Almost pure  $2H_1$  crystal was found in Nižná Slaná, and a totally disordered subfamily D crystal in the synthetic product.

EMPA revealed traces of Cl in samples from both localities (0.009 to 0.06 *apfu*), and of S (up to 0.11 *apfu*) in Nižná Slaná cronstedtite.

Now-a-days, the samples from Chyňava, and from Litošice-Sovolusky-Morašice region are under investigation.

1. J. Hybler, . Sejkora, V. Venclík, *Eur. J. Mineral.*, (2016), DOI: 10.1127/ejm/2016/0028-2532.
2. J. Hybler, M. Števkó, J. Sejkora, Accepted for publication in: *Eur. J. Mineral.* (2016).

3. I. Pignatelli, E. Mugnaioli, J. Hybler, R. Mosser-Ruck, M. Cathelineau, N. Michau, *Clay. Clay Miner.*, **61**, (2013), 277.
4. J. Hybler, *Acta Cryst.*, B70, (2014), 963.
5. J. Hybler, *Eur. J. Mineral.*, (2016), DOI:10.1127/ejm/2016/0028-2541

The study was supported by the grant 15-04204S of the Czech Science Foundation.

SL9

### Approximations of Fourier coefficients of diffractios profiles

## APROXIMACE FOURIEROVÝCH KOEFICIENTŮ DIFRAKČNÍCH PROFILŮ

M. Čerňanský

Fyzikální ústav AV ČR, Na Slovance 2, 182 21 Praha 8, Česká republika  
cernan@fzu.cz

Fourierovy koeficienty difrakčních profilů mají v práškové difrakci velký význam. Především mohou být využity k získání fyzikálního profilu z profilu měřeného a přístrojového [1]. Právě až fyzikální profil totiž obsahuje hledané informace o velikosti krystalitů, mikrodeformací a příp. dalších strukturálních poruchách. Warrenova – Averbachova [2] interpretace Fourierových koeficientů fyzikálních profilů, která umožňuje tyto informace získat, je založena na vztahu

$$A_n = \frac{N_n}{N_3} \langle \cos 2 l Z_n \rangle, \quad (1)$$

kde  $A_n$  je kosinusový koeficient Fourierovy řady difrakčního profilu linie 00*l* vzorku polykrystalu s ortorombickou mřížkou s parametry  $a_1$ ,  $a_2$ ,  $a_3$ . Dá se ukázat, že vhodnou transformací proměnných a souřadných os lze libovolnou reflexi *hkl* a libovolný souřadný systém převést na případ reflexe 00*l* v ortorombické soustavě [3].

V rovnici (1) je  $n$  pořadí Fourierového koeficientu,  $N_3$  je průměrný počet základních buněk ve sloupcích kolmých na difraktující roviny 00*l* (středuje se přes celý vzorek),  $N_n$  je průměrný počet sloupců sestávajících z  $n$  sousedících základních buněk (taky středováno přes celý vzorek),  $l$  je řád reflexe a  $Z_n$  je relativní změna vzdálenosti dvou základních buněk jednoho sloupce vlivem deformace. Absolutní změna má velikost  $L = Z_n a_3$ . V nedeformovaném stavu byla vzájemná vzdálenost těchto buněk  $L = n a_3$ . Mikrodeformace tedy je

$$n = \frac{L}{L} \frac{Z_n a_3}{n a_3} \frac{Z_n}{n}. \quad (2)$$

Podobně je zřejmé

$$N_3 a_3 = N_3 d = D, \quad (3)$$

kde  $D$  je průměrná velikost krystalických částic ve směru kolmém na difraktující roviny (00*l*) a  $d = a_3$  je meziorovinná vzdálenost (pro  $l = 1$ ).

Poměr  $(N_n/N_3)$  v (1) souvisí s velikostí krystalických částic, zřejmě nezávisí na řádu reflexe  $l$  a označuje se za velikostní Fourierův koeficient  $A_n^D$ . Pro malé hodnoty  $n$  platí dost přesně (např. [4]), že  $(N_n/N_3)$  se přibližně rovná  $[1 - (n/N_3)]$ , což lze považovat za první dva členy Taylorovy řady funkce  $\exp[-(n/N_3)]$ , takže

$$A_n^D = \frac{N_n}{N_3} \approx 1 - \frac{n}{N_3} \exp \frac{n}{N_3}. \quad (4)$$

Výraz  $\langle \cos 2 l Z_n \rangle$  – deformační Fourierův koeficient  $A_n$  – závisí na řádu reflexe  $l$  a pro malé hodnoty  $l$  a  $n$  ho lze aproximovat taky prvními dvěma členy jeho Taylorovy řady a ty pak opět lze považovat za první dva členy Taylorovy řady funkce  $\exp -2^2 l^2 \langle Z_n^2 \rangle$ , takže máme

$$A_n \langle \cos 2 l Z_n \rangle \approx 1 - 2^2 l^2 \langle Z_n^2 \rangle \exp -2^2 l^2 \langle Z_n^2 \rangle. \quad (5)$$

Aproximace (5) platí při malých hodnotách  $l$  a  $n$  pro libovolné statistické rozložení veličiny  $Z_n$ . Je-li toto rozložení Gaussovo, platí (5) pro libovolné hodnoty  $l$  a  $n$  přesně [2].

Pro výsledný Fourierův koeficient fyzikálního profilu  $A_n = A_n^D A_n$  pak z (1), (4) a (5) vyplývá

$$A_n = \exp \frac{n}{N_3} \exp -2^2 l^2 \langle Z_n^2 \rangle. \quad (6)$$

Protože podle (2) zřejmě je



$$\langle Z_n^2 \rangle = n^2 \langle \frac{2}{n} \rangle \frac{L}{d} \langle \frac{2}{n} \rangle, \quad (7)$$

vychází

$$A_n = \exp \frac{n}{N_3} \exp 2 \frac{2}{L^2 n^2} \langle \frac{2}{n} \rangle, \quad (8)$$

resp.

$$A_L = \exp(L/D) \exp KL^2 \langle \frac{2}{L} \rangle, \quad (9)$$

kde  $K = 2 \frac{2}{L^2}$  je pro danou difrakční linii konstanta a index Fourierového koeficientu  $n$  byl nahrazen vzdáleností  $L = na_3 = nd$ . U mikrodeformace se často uvádějí dolní indexy  $n$  nebo  $L$ , protože obecně na nich závisí. Nehomogenní deformace totiž zřejmě závisí na délce středování, resp. na délce podél které se určuje. Pokud se

předpokládá homogenní rozložení mikrodeformací, na  $n$  nezávisí a z (8) je

$$\ln A_n = Mn - Nn^2, \quad (10)$$

co znamená, že posloupnost logaritmu Fourierových koeficientů fyzikálního profilu lze aproximovat parabolou. Z jejích koeficientů  $M$  a  $N$  lze určit velikosti krystalitů a mikrodeformací, a to jenom z jedné difrakční linie [5]. Ke stejnému účelu byly navrženy další aproximační funkce, které budou uvedeny v příspěvku.

1. A. R. Stokes, *Proc. Phys. Soc.*, **61**, (1948), 382.
2. B. E. Warren, *Prog. Metal Phys.*, **8**, (1959), 146.
3. B. E. Warren, *Acta. Cryst.* **8**, (1955), 483.
4. R. Somashekar, I. H. Hall & P. D. Carr, *J. Appl. Cryst.*, **22**, (1989), 363.
5. B. Ja. Pines, *Dokl. AN SSSR*, **103**, (1955), 601.

SL10

## RESIDUAL STRESS DETERMINATION OF DUPLEX AND AUSTENITE STEELS MACHINED USING DIFFERENT TOOL GEOMETRY

J. Čapek<sup>1</sup>, K. Kolařík<sup>1</sup>, Z. Pitrmuc<sup>2</sup>, L. Beránek<sup>2</sup>, N. Ganev<sup>1</sup>

<sup>1</sup>Department of Solid State Engineering, Faculty of Nuclear Sciences and Physical Engineering, Czech Technical University in Prague

<sup>2</sup>Department of Machining, Process Planning and Metrology, Faculty of Mechanical Engineering, Czech Technical University in Prague

capekjir@fffi.cvut.cz

Duplex stainless steels have high corrosion resistance in many environments, where the standard austenite steel is consumed, and where its properties significantly exceed austenite steel. Duplex steels combine properties of both phases and moreover, due to two-phase microstructure, some properties are better than high-alloyed austenite steel, e.g. abrasion resistance [1]. Thereby, smaller amount of material from duplex steel is necessary to manufacture function components. Austenite and duplex steels are susceptible to mechanical reinforcement, i.e. local changes in mechanical properties of surface layers. Local changes, e.g. hardness, can lead to tools vibration during machining of the final component, which results in additional material inhomogeneity and blunting tool [2].

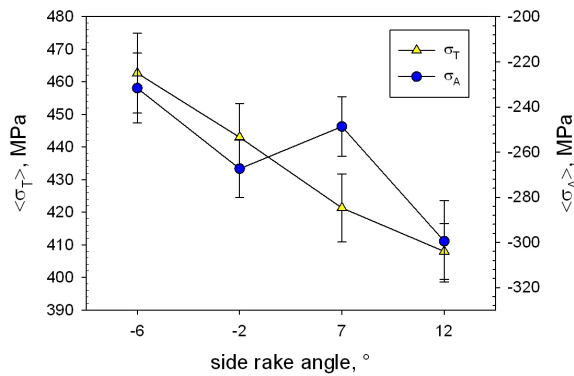
Realising that austenite steel has face centred cubic (fcc) lattice with close-packing structure of atoms, the primary slip system is  $\{111\}$ . The number of slip systems is 12, which is the sufficient amount to plastic deformation. Moving dislocations form so called stair-rod dislocations which have small stacking fault energy, i.e. high energy is necessary to have for intersect or cross slip of these dislocations [3]. Therefore, the austenite steels are prone to work-hardening, which cause mechanical modification and inhomogeneity on the machined surface, and leads to e.g. unstable chip formation. On the contrary, the ferrite crystallizes in a body centred cubic lattice (bcc). The direction slip in bcc materials is always  $\{110\}$ . Since in the bcc lattice is not close-packing structure of atoms, more

slip planes assert during the deformation, mostly planes  $\{110\}$  and  $\{211\}$ .

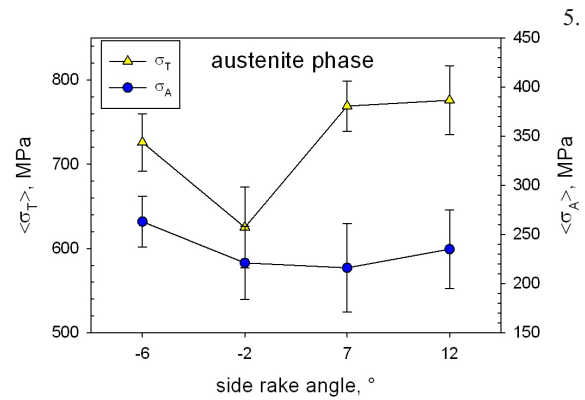
The tested samples of tube shape of 100/86 mm in diameter were made of AISI 304 (austenite) and AISI 318LN (duplex) type of stainless steel. The samples were annealed in air laboratory furnace for 5 hours at 420°C in order to reduce bulk macroscopic residual stresses. For machining of the surfaces, four types of side rake angle were used (-6°; -2°; +7° and +12°), namely F3M, SF, NF, and PP chip breakers of Iscar Cutting Tools.

Cutting conditions were as followed: feed rate 0.14 mm/rev, cutting speed 140 m/min, and depth of cut 2 mm. Direction of feed rate was parallel to axis of the sample (tube) A and perpendicular to tangential direction T. According to the principles of design of experiments (DOE) method, three 1cm tube segments were machined using the same cutting conditions.

Using MnK and CrK radiation, X'Pert PRO MPD diffractometer was used to measure lattice deformations in austenite and ferrite, respectively. Diffraction angles  $2\theta^{hkl}$  were determined from the peaks of the diffraction lines  $K_1$  of planes  $\{311\}$  and  $\{211\}$  of austenite and ferrite, respectively. In Figs. 1a-c, there are influences of surface macroscopic residual stresses  $\langle \sigma_A \rangle$ ;  $\langle \sigma_T \rangle$ , MPa on the side rake angle, °. These residual stresses were averaged from three values of RS of tube segments machined the same side rake angle.



a) Austenite steel.

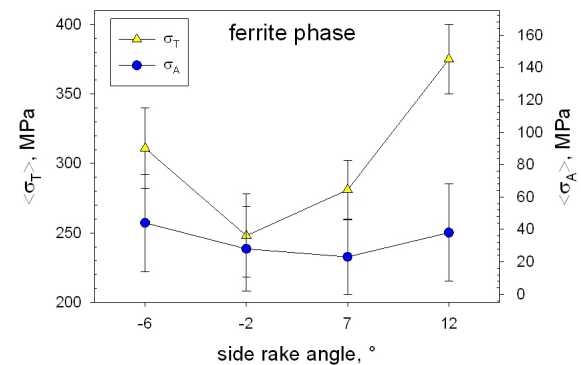


b) Duplex steel – austenite phase.

**Figure 1.** Axial and tangential residual stresses  $\langle \sigma_A \rangle$ ,  $\langle \sigma_T \rangle$  as a function of side rake angle.

Generally, the increasing of the side rake angle in the positive direction leads to a lowering of cutting force and temperature in the cutting zone [4]. For prediction of RS dependence on the side rake angle, the yield strength ratio  $R_m/R_{p0.2}$  of the given material is necessary to take into account. Generally, the temperature influence causes the tensile RS and contrarily, the plastic deformation leads to compressive RS. The type of the RS and their value deeply depend on the mechanical and thermal properties of the machined material [4, 5].

For austenite steel, higher compressive (axial direction) and smaller tensile (tangential direction) RS were determined with increasing of the side rake angle, see Fig. 1a. On the other hand, for ferrite steel, the greater force causes that the plastic deformation influence is predominant and higher compressive or smaller tensile RS may be determined with increasing of the side rake angle. Furthermore, for duplex steel, which is consisted of both phases, it is possible to presume that the dependence of RS on the side rake angle is generally not monotonic for both the phases because of their mutual influence during plastic deformation, see Figs. 1b-c.



c) Duplex steel – ferrite phase.

T. Leppert, R. L. Peng, *Produc. Eng.*, **6.4-5**, (2012), 367-374.

This work was supported by the Grant Agency of the Czech Technical University in Prague, grant No. SGS16/245/OHK4/3T/14.

1. R. Dakhlaoui, C. Braham, A. Baczmański, *Mater. Sci. Eng.: A*, **70.1**, (2007), 6-17.
2. J. Čapek, K. Kolařík, L. Beránek, A. Molotovník, N. Ganey, in *The 5th Student Scientific Conference on Solid State Physics*, edited by ČVUT Praha, 2005, pp. 11-15.
3. J. J. Moverare, M. Oden, *Mater. Sci. Eng.: A*, **337.1**, (2002), 25-38.
4. F. Neckář, I. Kvasnička, *Vybrané statě z úběru materiálu*. Praha: ČVUT. 1991.



SL11

## CONTRIBUTION TO STUDY OF Cu/Mn HETEROBIMETALLIC COMPOUNDS

E. Samolová, J. Kuchár

Department of Inorganic Chemistry, Institute of Chemistry, P. J. Šafárik University in Košice, Moyzesova 11,  
04154 Košice, Slovakia

erika.samolova@student.upjs.sk

Previously, it was demonstrated that besides the covalent bonds also hydrogen bonds (HBs) can be considered as additional paths for the magnetic exchange interactions [1, 2]. The study of magnetic and thermodynamic properties of structurally 1D compound  $\text{Cu}(\text{en})_2\text{Ni}(\text{CN})_4$  ( $\text{en}$  = ethane-1,2-diamine) in the low temperature region confirmed its magnetically 2D character, the present HBs of the  $\text{N-H}\cdots\text{N}$  type were suggested as additional exchange paths to the covalent bonds through the five-atomic  $-\text{NC-M-CN}$ -bridge [3]. Weak character of the magnetic exchange interactions is in line with long exchange path. We have undertaken a study of a series copper(II) compounds in which  $[\text{M}(\text{CN})_4]^{2-}$  bridging species with square coordinated diamagnetic M(II) atoms were replaced by  $[\text{MnCl}_4]^{2-}$  anion. The use of this anion allows the formation of Cu(II)-Mn(II) bimetallic chains with short bridge between the paramagnetic atoms consisted of one chloride ligand. These systems are interesting from magnetic point of view, chains of Mn(II) ( $S = 5/2$ ) and Cu(II) ( $S = 1/2$ ) structurally ordered in an alternating manner are of intense interest as potential starting blocks in the synthesis of molecular-based ferromagnets [4].

We have prepared and structurally characterized three novel compounds using the methyl derivatives of ethylenediamine:  $\text{Cu}(\text{men})_2\text{MnCl}_4$  (**1**),  $\text{Cu}(\text{bmen})_2\text{MnCl}_4$  (**2**) and  $\text{Cu}(\text{dmen})_2\text{MnCl}_4$  (**3**) ( $\text{men}$  = N-methylethane-1,2-diamine;  $\text{bmen}$  = N,N'-dimethylethane-1,2-diamine;  $\text{dmen}$  = N,N-dimethylethane-1,2-diamine). Compounds **1** and **2**

exhibit chain-like structures analogous to the already reported  $\text{Cu}(\text{en})_2\text{MnCl}_4$  [5] in which alternating Cu(II) and Mn(II) atoms are bridged by chloride ligand. The hexa-coordinated Cu(II) atom is surrounded by two chelate bonded blocking ligands and two chloride ligands are placed in the trans positions, the Mn(II) coordination environment approximates tetrahedral symmetry. On the other hand, the use of the unsymmetrical  $\text{dmen}$  ligand leads to a dinuclear compound **3** with molecular structure in which the pentacoordinated Cu(II) and tetrahedrally coordinated Mn(II) atoms are linked by one bridging chlorido ligand. Further details on the syntheses, characterizations and crystal structures will be given.

1. J. Kuchár, J. Černák, Z. Mayerová, P. Kubáček, Z. Žák, *Solid State Phenom.*, **90-91**, (2003), 328.
2. E. Čižmár, A. Orendáčová, M. Orendáč, J. Kuchár, M. Vavra, I. Potočňák, J. Černák, E. Casini, A. Feher, *Phys. Status Sol. B*, **243**, (2006), 268.
3. M. Orendáč, A. Orendáčová, J. Černák, A. Feher, *Solid State Commun*, **94**, (1995), 833.
4. H. O. Stumpf, Y. Pei, O. Kahn, J. Sletten, J. P. Renard, *J. Am. Chem. Soc.*, **115**, (1993), 6738.
5. B. Chiari, A. Cinti, O. Piovesana, P. F. Zanazzi, *Inorg Chem.*, **34**(10)(1995), 34(10), 2652.

This work was supported by P. J. Šafárik University in Košice (VVGS-PF-2016-72623, VVGS-2016-265).

SL12

## SYNTHESIS, CHARACTERIZATION AND CRYSTAL STRUCTURES OF TWO POLYMORPHS OF $[\text{Co}_2(\text{o-van-en})_3]\cdot 4\text{CH}_3\text{CN}$

A. Vráblová<sup>1</sup>, J. Černák<sup>1</sup>, L. Falvello<sup>2</sup>, M. Tomás<sup>2</sup>

<sup>1</sup>Department of Inorganic Chemistry, Institute of Chemistry, P. J. Šafárik University in Košice, Moyzesova 11,  
041 54 Košice, Slovakia

<sup>2</sup>Facultad de Ciencias, Universidad de Zaragoza, Pedro Cerbuna 12, 50009 Zaragoza, Spain  
anna.vrablova@student.upjs.sk

Schiff bases are often used as ligands for the coordination of cobalt due to their multi-donor properties [1] and consequent versatility. In our quest for Co(II) complexes as magnetically active materials [2; 3] we have isolated two polymorphs of  $[\text{Co}_2(\text{o-van-en})_3]\cdot 4\text{CH}_3\text{CN}$  (**1** and **2**) based on the Schiff base ligand *o-van-en* synthesized by the reaction of ethylenediamine with *o*-vanillin in 1:2 molar ratio (Scheme 1).

The triclinic (P-1) polymorph **1** was obtained after room temperature crystallization of the acetonitrile solu-

tion of the reaction product of the Schiff base with cobalt hydroxide in air. Differences in reaction and crystallization conditions produced the monoclinic form **2** (space group  $P2_1/c$ ). Both polymorphs were chemically and spectroscopically characterized, and the results indicated spontaneous oxidation of Co(II) to Co(III). The crystal structures of both **1** and **2** are built up of molecules of the centrosymmetric dinuclear complex  $[\text{Co}_2(\text{o-van-en})_3]$ , in which each Co(III) atom is coordinated by one tetradentate *o-van-en* ligand in an uncommon bent fashion. The

pseudooctahedral coordination of the Co(III) atom is completed by one phenolato O and one amidic N atom of the same arm of the bridging *o-van-en* ligand. In addition, the asymmetric units of both polymorphs contain two acetonitrile solvate molecules. In polymorph **2**, consistent with the symmetry of the space group, the dinuclear  $\{Co_2\}$  units are arranged in an alternating ABABAB fashion, in contrast to the AAA arrangement of the dinuclear units in polymorph **1**. As a consequence, both polymorphs differ in the positions of the acetonitrile solvate molecules and in the pattern of intermolecular interactions. Differences of some geometrical parameters, e.g., torsion angles were observed, too.

1. M. Andruh, *Dalton Trans.*, **44**, (2015), 16633-16653.
2. E. Burzurí, J. Campo, L. R. Falvello, E. Forcén-Vázquez, F. Luis, I. Mayoral, F. Palacio, C. Sáenz de Pipaón, M. Tomás, *Chem. Eur. J.*, **17**, (2011), 2818-2822.

## Session VIII, Thursday, September 15

L20

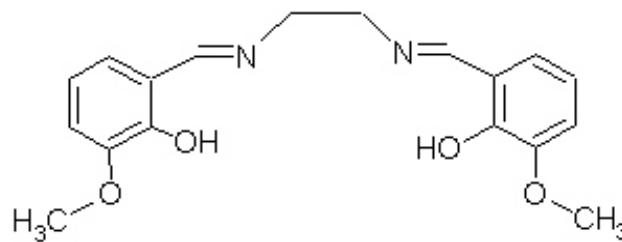
### ELECTRON BACKSCATTER DIFFRACTION - EBSD

Milan Dopita

*Department of Condensed Matter Physics, Faculty of Mathematics and Physics,  
Charles University in Prague, dopita@gmail.com*

The electron backscatter diffraction (EBSD) is the method widely used in materials science, nowadays. In past twenty years the instrumentation underwent extensive progress and the EBSD became standard laboratory technique. Significant progress in the instrumentation, the development of modern high resolution scanning electron microscopes and dual beam microscopes, as well as the fast EBSD detectors still offers the new possibilities of application of EBSD method for studying of various types of modern and perspective materials.

The Kikuchi pattern formation in Transmission Electron Microscope (TEM) was first observed and explained in 1928 by S. Kikuchi [1]. It was immediately found that the Kikuchi pattern is a powerful tool for the crystal orientation determination because "The Kikuchi diffraction pattern is a projection of the geometry of the crystal lattice from a volume of specimen in which this geometry is constant, or nearly so (Kikuchi [1])." In 1932 Meibon and Rupp observed high angle Kikuchi patterns from "reflected" electrons. Venables and Harland observed electron backscatter patterns in the Scanning Electron Microscope equipped with 30 mm diameter fluorescent imaging screen and television camera. This method allowed examination of specimens and the measurement of crystal orientation at high spatial resolution, which was significantly improved by the use of field emission gun scanning electron microscopes. The first on-line working (automated) EBSD systems were developed in 1980. In 1993 the Orientation Imaging Microscopy (OIM) or orientation mapping was established. The on-line orientation determination from the EBSD patterns is computationally time-



**Scheme 1.** Structural diagram of  $H_2(o\text{-van-en})$ .

3. L. Smolko, J. Černák, J. Kuchár, J. Miklovič, R. Boča, *J. Mol. Structure*, **1119**, (2016), 437-441.

*This work was supported by P. J. Šafárik University in Košice (VVGS-PF-2016-72623, VVGS-2016-265). The stay of AV in University of Zaragoza was supported by National Scholarship Programme of the Slovak Republic.*

consuming task, however within the last decades the EBSD technique underwent a great boom as a consequence of the computers hardware improvements and progresses in the scanning electron microscopes technique, as well.

The EBSD is surface sensitive method. Measured information come from the depth of several tenths of nm, depending on the measured material atomic number (the penetration depth of electrons decreases with increasing atomic number). The spatial resolution of the EBSD depends on the used electron microscope type (used electron source). In the case of scanning electron microscope equipped with field emission cathode it is in order of  $\sim 10$  nm.

Two types of information are essentially held by the electron backscatter patterns. First is the Kikuchi pattern quality measure and the second is the orientation of irradiated volume. The Kikuchi pattern quality information, can be used for determination of the crystal "perfection", estimation of the crystal defects types and its densities because the presence of the lattice defects in irradiated volume has in general in consequence decrease of the Kikuchi pattern "sharpness" (blurring of the Kikuchi pattern). However, the Kikuchi pattern quality is strongly influenced by the specimen surface preparation. The surface area is in most cases of samples highly defective (from production or sample processing). The Kikuchi pattern from poorly prepared specimen is therefore not sharp and this effect correlates with influence of the lattice defects and imperfections. Therefore, the determination of the lattice defects and densities can be done only quasi-quantitatively.